

Dipolar mode localization and spectral gaps in quasi-periodic arrays of ferromagnetic nanoparticles

Carlo Forestiere, Giovanni Miano, and Claudio Serpico

Department of Electrical Engineering, Università degli Studi di Napoli Federico II, Napoli 80125, Italy

Massimiliano d'Aquino

Department of Technology, Università di Napoli Parthenope, Napoli 80143, Italy

Luca Dal Negro

Department of Electrical and Computer Engineering and Division of Materials Science and Engineering, Boston University, Boston, Massachusetts 02215, USA

(Received 11 March 2009; revised manuscript received 16 May 2009; published 15 June 2009)

In this paper we study the spectral, localization, and dispersion properties of the ferromagnetic dipolar modes around a stable, saturated, and spatially uniform equilibrium in quasi-periodically modulated arrays of ferromagnetic nanoparticles based on the Fibonacci sequence. The Fibonacci sequence is the chief example of deterministic quasi-periodic order. The problem is reduced to the study of a linear-generalized eigenvalue equation for a suitable Hermitian operator connected to the micromagnetic effective field, which accounts for the magnetostatic, anisotropy, and Zeeman interactions. The coupling with a weak applied magnetic field, varying sinusoidally in time, is dealt with and the role of the losses is highlighted. By calculating the resonance frequencies and eigenmodes of the Fibonacci arrays we demonstrate the presence of large spectral gaps and strongly localized modes and we evaluate the pseudodispersion diagrams. The magnetization oscillation modes in quasi-periodic arrays of magnetic nanoparticles show, at microwave frequencies, behaviors that are very similar to those shown, at optical frequencies, by plasmon modes in quasi-periodic arrays of metal nanoparticles. The presence of band gaps and strongly localized states in magnetic nanoparticle arrays based on quasi-periodic order may have an impact in the design and fabrication of new microwave nanodevices and magnetic nanosensors.

DOI: [10.1103/PhysRevB.79.214419](https://doi.org/10.1103/PhysRevB.79.214419)

PACS number(s): 76.50.+g, 75.75.+a, 75.10.Pq

I. INTRODUCTION

As lithographic techniques have rapidly developed in the last decade, it has become possible to assemble ordered magnetic elements on the nanometer scale (e.g., Ref. 1). Patterned arrays of single-domain nanoparticles are the subject of substantial current research interest due to their potential applications, for example, in future magnetic data storage, new magnetic-sensing devices, and new microwave devices (e.g., Refs. 2 and 3). Mode excitations control the dynamic response of the magnetization in the linear regime and the speed of real devices at least for small amplitude motions of the magnetization. The presence of large band gaps in the magnetization response may have large impacts in the development of new microwave devices, for example, microwave filters. Highly localized magnetization oscillation modes, with strong near-field enhancement, may have a significant influence in the design and fabrication of new magnetic nanosensors and nanoscale magnetometers (tomography and magnetic imaging).

In patterned array the dipolar interaction among particles strongly affects the mode distributions and their resonance frequencies. This provides motivation for theoretical and experimental studies of the magnetization oscillation modes in array of magnetic nanoparticles. Considerable attention has been given lately to the oscillation modes of periodic array of magnetic nanoparticles (e.g., Refs. 4–8).

Quasi-periodic order has an important role in many domains of science and technology (e.g., Refs. 9–13). The con-

trol of the electromagnetic field-matter interaction in deterministic arrays of nanoparticles without translational invariance offers an almost unexplored potential for the creation and manipulation of high-intensity electromagnetic fields that are confined in regions of space with dimensions much smaller than the characteristic wavelength and the transport of electromagnetic waves. Deterministic quasi-periodic arrays share distinctive physical properties with both periodic media, i.e., the formation of well-defined energy gaps, and disordered random media, i.e., the presence of localized eigenstates with high-field enhancement. Unlike random media, deterministic quasi-periodic structures are defined by the iteration of simple inflation rules, which offer a high degree of complexity combined with reproducibility. Until now, the study of the interaction of the electromagnetic field with deterministic aperiodic structures has been mainly directed to dielectric or magnetic multilayers (e.g., Ref. 10), aperiodic photonic crystals (e.g., Ref. 11), and arrays of metallic nanoparticles (Refs. 12–14). In particular, light scattering, plasmon localization, and band-gap formation in one- and two-dimensional arrays of metal nanoparticles with deterministic aperiodic geometries have been recently discussed (Refs. 12–15). However, the impact of the quasi-periodicity on the transport of magnetization oscillation modes and on the localization properties of quasi-periodic-based magnetic nanodevices has not been addressed so far.

In this paper we study the spectral, localization, and dispersion characteristics of the dipolar modes around a stable,

saturated, and spatially uniform equilibrium, in a Fibonacci chain of ferromagnetic nanoparticles, and their coupling with an applied time harmonic weak magnetic field. The distance between the nanoparticles is modulated according to the Fibonacci sequence (e.g., Ref. 12). This sequence represents the chief example of the quasi-periodic order characterized by quasi-periodic Fourier spectra. We demonstrate the presence of several band gaps and localized states, similarly to what happens for the plasmon modes in arrays of metallic nanoparticles.^{12,14} In quasi-periodic metal nanoparticle arrays, spectral gaps and mode localization arise in the optical frequency range; instead in quasi-periodic magnetic nanoparticle arrays they arise in the microwave frequency range. Furthermore, in quasi-periodic magnetic nanoparticle arrays the gaps may be widened by reducing the applied equilibrium magnetic field. In this way we may obtain gap widths, normalized to the Kittel frequency, much greater than the plasmonic gap widths, normalized to the plasmon frequency. As far as we know only aperiodic multilayers of magnetic materials have been considered until now (e.g., Ref. 10). Some preliminary results have been given in Ref. 16. There are many differences between an aperiodic array of magnetic nanoparticles and an aperiodic sequence of magnetic layers. In deterministic aperiodic nanoparticle arrays the dipolar interactions, depending on the distances between the nanoparticles, determine the main properties of the dipolar modes. Furthermore, the magnetic field near the nanoparticles, which may be very intense and strongly localized, is directly accessible.

The magnetization field density induced by the weak external magnetic field is assumed to be uniform in each nanoparticle and its dynamic is described by representing each nanoparticle as a point magnetic dipole. The dynamics of the magnetic dipoles are described by a discrete version of the linearized Landau Lifshitz-Gilbert equation. The study of the properties of the dipolar modes is reduced to the study of the spectral properties of a generalized eigenvalue problem related with a Hermitian matrix expressing the intensity of the magnetic field at the nanoparticle centers as functions of the magnetic dipole moments.

The paper is organized as follows. In Sec. II we formulate the equations governing the magnetization oscillations, around a saturated, stable, and spatially uniform equilibrium, in an array of magnetic nanoparticles. In Sec. III we discuss the main properties of the generalized eigenvalue problem governing the dipolar modes of the system. In Sec. IV we deal with the coupling problem with a weak external magnetic field, varying sinusoidally in time. In Sec. V we study the dipolar modes excited in a linear quasi-periodic chain generated according to the Fibonacci sequence. In Sec. VI we summarize our findings and draw our conclusions.

II. DIPOLAR MODEL

In this section we will introduce the model used for the analysis of the magnetization oscillations around a saturated, stable, and spatially uniform equilibrium in arrays of magnetic nanoparticles. The nanoparticles are all equal and with spherical shapes. To model the magnetization dynamics we

assume that the radius a of the spheres is smaller than the interparticle distance and comparable with the exchange length; the largest linear dimension of the array is much less than the characteristic wavelength of the electromagnetic field. As consequence we have that the magnetization field density may be assumed almost uniform in each nanoparticle; the magnetic field generated by the magnetization of each nanoparticle is mainly that generated by its magnetic dipole moment and it is almost uniform in the nanoparticles; the magnetic-field dynamics are governed by the magnetic quasi-stationary approximation of the Maxwell equations. Therefore, we shall study the magnetization oscillations of the array by modeling each magnetic nanoparticle as a point magnetic dipole and considering only the quasi-static contribution to the electromagnetic interaction between the magnetic dipoles. These assumptions are valid as long as the interparticle separation is at least equal to the radius of the particles and the radius of the particles is comparable than the exchange length.¹⁷ If the interparticle separation is less than the particle radius the effects of high-order moments of the magnetization density may become important and the magnetization dynamics are no longer governed only by the dipolar interaction. Therefore, the theory that we develop in this paper is valid only under the assumption that the interparticle separation is at least equal to the nanoparticle radius.

Let us consider an array of N magnetic nanoparticles. We denote with: $\mathbf{r}_1, \mathbf{r}_2, \dots, \mathbf{r}_N$ as the position vectors of the nanoparticle centers with respect to an assigned reference point; $\mathbf{M}_1, \mathbf{M}_2, \dots, \mathbf{M}_N$ as the magnetization densities of the nanoparticles; $\mathbf{H}^{(m)} = \mathbf{H}^{(m)}(\mathbf{r}; t)$ as the magnetic field generated by the nanoparticle magnetization; $\mathbf{H}^{(e)} = \mathbf{H}_0^{(e)} + \delta\mathbf{H}^{(e)}(t)$ as the external magnetic field, uniformly distributed along the array, where $\mathbf{H}_0^{(e)}$ is the equilibrium term and $\delta\mathbf{H}^{(e)}$ is a perturbation term that varies sinusoidally in time, $\delta\mathbf{H}^{(e)}(t) = \text{Re}\{\delta\mathbf{H}_M^{(e)} e^{i\omega t}\}$. We measure the time in units of $(\gamma M_S)^{-1}$ and introduce the dimensionless variables

$$\mathbf{m}_h \equiv \frac{1}{M_S} \mathbf{M}_h, \quad \mathbf{h}_h^{(m)} \equiv \frac{1}{M_S} \mathbf{H}^{(m)}(\mathbf{r} = \mathbf{r}_h, t), \quad (1)$$

$$\mathbf{h}_0^{(e)} \equiv \frac{1}{M_S} \mathbf{H}_0^{(e)}, \quad \delta\mathbf{h}^{(e)} \equiv \frac{1}{M_S} \delta\mathbf{H}^{(e)},$$

where $h = 1, 2, \dots, N$, M_S is the saturation magnetization, and γ is the absolute value of the gyromagnetic ratio (for electron spin $\gamma = 2.21 \times 10^5 \text{ mA}^{-1} \text{ s}^{-1}$).

The magnetization dynamics are governed by the system of equations

$$\frac{d\mathbf{m}_h}{dt} = -\mathbf{m}_h \times \left\{ \mathbf{h}_h^{(m)} + \kappa_{\text{an}}(\mathbf{e} \cdot \mathbf{m}_h)\mathbf{e} + [\mathbf{h}_0^{(e)} + \delta\mathbf{h}^{(e)}(t)] \right. \\ \left. - \alpha \frac{d\mathbf{m}_h}{dt} \right\} \text{ for } h = 1, 2, \dots, N, \quad (2)$$

where $\kappa_{\text{an}} > 0$ and \mathbf{e} are the normalized uniaxial anisotropy constant and unit vector, respectively, α is the Gilbert damping constant ($\alpha \leq 10^{-2}$),

$$\mathbf{h}_h^{(m)} = \mathcal{H}_h(\mathbf{m}_1, \mathbf{m}_2, \dots, \mathbf{m}_N) \equiv -\frac{1}{3}\mathbf{m}_h + \frac{1}{3} \sum_{\substack{k=1 \\ k \neq h}}^M \left(\frac{a}{|\mathbf{r}_h - \mathbf{r}_k|} \right)^3 \mathcal{A}_{hk} \mathbf{m}_k. \quad (3)$$

\mathcal{A}_{hk} is the dyad defined as

$$\mathcal{A}_{hk} = 3 \frac{\mathbf{r}_h - \mathbf{r}_k}{|\mathbf{r}_h - \mathbf{r}_k|} \otimes \frac{\mathbf{r}_h - \mathbf{r}_k}{|\mathbf{r}_h - \mathbf{r}_k|} - I, \quad (4)$$

\otimes is the tensor product and I is the identity operator. The system of Eq. (2) has to be solved with the constraint $|\mathbf{m}_h(t)|=1$ for $h=1, 2, \dots, N$.

At equilibrium, that is, for $\delta\mathbf{h}^{(e)}=\mathbf{0}$, we assume that all the nanoparticles are saturated along the direction \mathbf{e} by a strong-applied uniform magnetic field

$$\mathbf{h}_0^{(e)} = h_0 \mathbf{e}, \quad (5)$$

(or, equivalently, by a strong uniaxial anisotropy) and the magnetization is the same in each nanoparticle

$$\mathbf{m}_{0h} = \mathbf{e} \text{ for } h=1, 2, \dots, N. \quad (6)$$

Furthermore, we assume that this equilibrium configuration is stable.

The weak applied magnetic field induces a perturbation of the magnetization such that

$$\mathbf{m}_h(t) = \mathbf{e} + \text{Re}\{\delta\mathbf{m}_h e^{i\omega t}\} \text{ for } h=1, 2, \dots, N, \quad (7)$$

where $\delta\mathbf{m}_h$ is a complex constant vector such that $|\delta\mathbf{m}_h| \ll 1$ and $\delta\mathbf{m}_h \cdot \mathbf{e} = 0$. By substituting Eq. (7) in Eq. (2), by linearizing it around the equilibrium configuration, and by projecting the resulting expression in the plane orthogonal to \mathbf{e} , we obtain the equations governing the frequency domain linear response of the system

$$i\omega(\mathcal{R}\{\delta\mathbf{w}\} + \alpha\delta\mathbf{w}) - \mathcal{L}\{\delta\mathbf{w}\} = \delta\mathbf{h}_M^{(e)}, \quad (8)$$

where $\delta\mathbf{w} \in \mathbb{C}^{2N}$ is the complex vector

$$\delta\mathbf{w} = |\delta\mathbf{m}_1, \delta\mathbf{m}_2, \dots, \delta\mathbf{m}_N|^T, \quad (9)$$

$\mathcal{L}: \mathbb{C}^{2N} \rightarrow \mathbb{C}^{2N}$ is the linear operator represented columnwise

$$\mathcal{L}\{\delta\mathbf{w}\} = |\mathcal{L}_1\{\delta\mathbf{w}\}, \mathcal{L}_2\{\delta\mathbf{w}\}, \dots, \mathcal{L}_N\{\delta\mathbf{w}\}|, \quad (10)$$

with

$$\mathcal{L}_h\{\delta\mathbf{w}\} = -\mathbf{e} \times [\mathbf{e} \times \mathcal{H}_h(\delta\mathbf{w})] - h_{0h} \delta\mathbf{m}_h, \quad (11)$$

and

$$h_{0h} = \mathcal{H}_h(\mathbf{e}, \mathbf{e}, \dots, \mathbf{e}) \cdot \mathbf{e} + (h_0 + \kappa_{\text{an}}), \quad (12)$$

$\mathcal{R}: \mathbb{C}^{2N} \rightarrow \mathbb{C}^{2N}$ is the complex linear operator

$$\mathcal{R}\{\delta\mathbf{w}\} = \text{diag}\{\mathcal{R}_e\{\delta\mathbf{m}_1\}, \mathcal{R}_e\{\delta\mathbf{m}_2\}, \dots, \mathcal{R}_e\{\delta\mathbf{m}_N\}\}, \quad (13)$$

and $\mathcal{R}_e: \mathbb{C}^2 \rightarrow \mathbb{C}^2$ is the rotation dyad

$$\mathcal{R}_e\{\delta\mathbf{m}_h\} = \mathbf{e} \times \delta\mathbf{m}_h, \quad (14)$$

$\delta\mathbf{h}_M^{(e)} \in \mathbb{C}^{2N}$ is the known complex vector

$$\delta\mathbf{h}_M^{(e)} = \frac{1}{M_s} |\delta\mathbf{H}_M^{(e)}, \delta\mathbf{H}_M^{(e)}, \dots, \delta\mathbf{H}_M^{(e)}|^T. \quad (15)$$

The linear operator \mathcal{R} is antihermitian and the linear operator \mathcal{L} is Hermitian. Since the quadratic form $-\delta\mathbf{w}^T \mathcal{L}\{\delta\mathbf{w}\}$ is equal to half of the second variation in the free energy of the system, the linear operator $-\mathcal{L}$ is strictly positive for stable equilibria.¹⁸

III. MODAL ANALYSIS

The behavior of the solutions of Eq. (8) depends strongly on the natural oscillations of the system, that is, the solutions of the equation

$$\mathcal{L}\{\mathbf{u}\} = i\omega(\mathcal{R}\{\mathbf{u}\} + \alpha\mathbf{u}). \quad (16)$$

The natural frequencies are the eigenvalues of generalized eigenvalue problem (16) and the natural modes are the corresponding eigenvectors. If ω is an eigenvalue $-\omega^*$ is an eigenvalue, as well; the eigenvector corresponding to $-\omega^*$ is the complex conjugate of the eigenvector \mathbf{u} corresponding to the eigenvalue ω . We introduce then the notation

$$\omega_{-n} = -\omega_n^*, \mathbf{u}_{-n} = \mathbf{u}_n^* \text{ for } n=1, 2, \dots, N, \quad (17)$$

where $\omega_1, \omega_2, \dots, \omega_N$ is the set of eigenvalues with positive real parts, ordered in such a way that $\text{Re}\{\omega_1\} \leq \text{Re}\{\omega_2\} \leq \dots \leq \text{Re}\{\omega_N\}$.

Let us introduce the following scalar products in \mathbb{C}^{2N}

$$\langle \mathbf{a}, \mathbf{b} \rangle = -\mathbf{a}^\dagger \mathcal{L}\{\mathbf{b}\} \text{ and } \langle \mathbf{a}, \mathbf{b} \rangle = \mathbf{a}^\dagger \mathbf{a}. \quad (18)$$

We normalize the eigenvectors in such a way that

$$\langle \mathbf{u}_n, \mathbf{u}_n \rangle = 1 \quad (19)$$

for any n . By using the properties of \mathcal{L} and \mathcal{R} from the generalized eigenvalue problem (16), it follows

$$\frac{\omega_n - \omega_n^*}{\omega_n + \omega_n^*} = i\alpha\omega_n \frac{\langle \mathbf{u}_n, \mathbf{u}_n \rangle}{1 + i\alpha\omega_n \langle \mathbf{u}_n, \mathbf{u}_n \rangle}, \quad (20)$$

$$\langle \mathbf{u}_m, \mathbf{u}_n \rangle = 2\alpha i \frac{\omega_m^* \omega_n}{\omega_m^* - \omega_n} \langle \mathbf{u}_m, \mathbf{u}_n \rangle \text{ for } m \neq n. \quad (21)$$

From these relations it results that the eigenfrequencies are real and positive in the lossless limit $\alpha=0$; the eigenmodes are orthonormal with respect to the scalar product $\langle \mathbf{a}, \mathbf{b} \rangle$ in the lossless limit $\alpha=0$.

Since $\alpha \ll 1$ the eigenvalues and eigenvectors of the generalized eigenvalue problem (16) may be evaluated by using the perturbation theory. We may express the eigenvalue ω_h and the corresponding eigenvector \mathbf{u}_n as

$$\omega_n = \omega_n^{(0)} + \alpha\omega_n^{(1)} + O(\alpha^2), \quad (22)$$

$$\mathbf{u}_n = \mathbf{u}_n^{(0)} + \alpha\mathbf{u}_n^{(1)} + O(\alpha^2), \quad (23)$$

where $\omega_n^{(0)}$ and $\mathbf{u}_n^{(0)}$ are, respectively, the h th natural frequency and the corresponding natural mode in the lossless limit $\alpha=0$, and $\omega_n^{(1)}$ and $\mathbf{u}_n^{(1)}$ take into account the first-order corrections in the small parameter α .

By substituting expressions (22) and (23) in relation (20), and by disregarding all the terms of order higher than one, we obtain the following expressions for the first-order correction terms

$$\omega_n^{(1)} = i\mu_n \text{ for } n = 1, 2, \dots, N, \quad (24)$$

$$\mathbf{u}_n^{(1)} = \sum_{m=1}^N [c_{nm}\mathbf{u}_m^{(0)} + c_{n,-m}\mathbf{u}_{-m}^{(0)}] \text{ for } n = 1, 2, \dots, N, \quad (25)$$

where

$$\mu_n = (\omega_n^{(0)})^2 \langle \mathbf{u}_n^{(0)}, \mathbf{u}_n^{(0)} \rangle > 0, \quad (26)$$

$$c_{nm} = i\alpha \begin{cases} \frac{1}{2} \langle \mathbf{u}_n^{(0)}, \mathbf{u}_m^{(0)} \rangle & \text{for } n = m, \\ \frac{\omega_n^{(0)}}{\omega_m^{(0)} - \omega_n^{(0)}} \langle \mathbf{u}_n^{(0)}, \mathbf{u}_m^{(0)} \rangle & \text{for } n \neq m. \end{cases} \quad (27)$$

IV. COUPLING WITH THE EXTERNAL FIELD

We look for the solution of Eq. (8) by representing $\delta\mathbf{w}$ in terms of the natural modes of the system

$$\delta\mathbf{w} = \sum_{n=1}^N (a_n \mathbf{u}_n + a_{-n} \mathbf{u}_{-n}), \quad (28)$$

where the coefficients a_k are unknown and are to be determined by imposing that expression (28) satisfies Eq. (8). By substituting expression (28) in Eq. (8) and by using Eq. (16), we have

$$\sum_{n=1}^N \left[\left(\frac{\omega}{\omega_n} - 1 \right) a_n \mathcal{L}\{\mathbf{u}_n\} + \left(\frac{\omega}{\omega_{-n}} - 1 \right) a_{-n} \mathcal{L}\{\mathbf{u}_{-n}\} \right] = \delta\mathbf{h}_M^{(e)}. \quad (29)$$

By multiplying on the left both members of Eq. (29) first by \mathbf{u}_{+n}^\dagger and then by \mathbf{u}_{-n}^\dagger , we finally obtain the system of linear equations

$$\begin{aligned} \sum_{m=1}^N \left[\left(1 - \frac{\omega}{\omega_m} \right) \langle \mathbf{u}_n, \mathbf{u}_m \rangle a_m + \left(1 - \frac{\omega}{\omega_{-m}} \right) \langle \mathbf{u}_n, \mathbf{u}_{-m} \rangle a_{-m} \right] &= \langle \mathbf{u}_n, \delta\mathbf{h}_M^{(e)} \rangle \\ \sum_{m=1}^N \left[\left(1 - \frac{\omega}{\omega_m} \right) \langle \mathbf{u}_{-n}, \mathbf{u}_m \rangle a_m + \left(1 - \frac{\omega}{\omega_{-m}} \right) \langle \mathbf{u}_{-n}, \mathbf{u}_{-m} \rangle a_{-m} \right] &= \langle \mathbf{u}_{-n}, \delta\mathbf{h}_M^{(e)} \rangle \end{aligned} \quad \text{for } n = 1, 2, \dots, N. \quad (30)$$

Since $\alpha \ll 1$ it results $|\langle \mathbf{u}_n, \mathbf{u}_m \rangle| \ll 1$ for $n \neq m$ and the system of Eq. (30) may be strongly simplified by setting $\langle \mathbf{u}_n, \mathbf{u}_m \rangle = \delta_{nm}$. In this way we obtain a system of uncoupled equations and

$$\begin{aligned} a_n &\cong \frac{\omega_n}{\omega_n - \omega} \langle \mathbf{u}_n, \delta\mathbf{h}_M^{(e)} \rangle \\ a_{-n} &\cong -\frac{\omega_n^*}{\omega_n^* + \omega} \langle \mathbf{u}_n^*, \delta\mathbf{h}_M^{(e)} \rangle \end{aligned} \quad \text{for } n = 1, 2, \dots, N. \quad (31)$$

By taking into account these properties and by substituting expressions (31) in sum (28), we obtain for $\delta\mathbf{w}$

$$\delta\mathbf{w} \cong \sum_{n=1}^N \left[\frac{\omega_n}{\omega_n - \omega} \langle \mathbf{u}_n, \delta\mathbf{h}_M^{(e)} \rangle \mathbf{u}_n - \frac{\omega_n^*}{\omega_n^* + \omega} \langle \mathbf{u}_n^*, \delta\mathbf{h}_M^{(e)} \rangle \mathbf{u}_n^* \right]. \quad (32)$$

Only the first term may give rise to resonances. The applied magnetic field is in resonance with the n th mode at the frequency ω for which the mode response function of the n th mode,

$$A_n(\omega) = \left| \frac{\omega_n}{\omega_n - \omega} \right| \cong \left| \frac{\omega_n^{(0)} + i\alpha\mu_n}{(\omega_n^{(0)} - \omega) + i\alpha\mu_n} \right|, \quad (33)$$

is maximum. The resonance frequency is, with good approximation, equal to the lossless natural frequency $\omega_n^{(0)}$. The 3 dB bandwidth $\Delta\omega$ of the response function $A_n(\omega)$ is equal to $2\alpha\mu_n$ and the quality factor Q_n is equal to $A_n(\omega_n^{(0)}) \cong 2\omega_n^{(0)}/\Delta\omega$. By using expression (26) we obtain

$$\Delta\omega = 2\alpha(\omega_n^{(0)})^2 \langle \mathbf{u}_n^{(0)}, \mathbf{u}_n^{(0)} \rangle, \quad (34)$$

$$Q_n = \frac{1}{\alpha} \frac{1}{\omega_n^{(0)} \langle \mathbf{u}_n^{(0)}, \mathbf{u}_n^{(0)} \rangle}. \quad (35)$$

The selectivity of the coupling between the array and the time-varying external magnetic field depends on the 3 dB bandwidth of the mode response functions, and it is limited by the losses and by the difference between the resonance frequencies of the modes. Spin-momentum transfer can be used to compensate the damping^{19,20} and equivalent values of α of the order of 10^{-3} may be obtained.

V. FIBONACCI LINEAR CHAINS

We now study in detail the spectral properties of the quasi-periodic linear chains of magnetic nanoparticles based

on the Fibonacci sequence. As already stated, the Fibonacci sequence represents the chief example of deterministic aperiodic systems, characterized by quasi-periodic Fourier spectra. The set of distances between adjacent particles is composed of two values denoted with d_A and d_B . We shall assume in a conventional way $d_B \geq d_A$. The sequence of symbols d_A and d_B are generated according to the Fibonacci inflation rule: $A \rightarrow AB$ and $B \rightarrow A$ (e.g., Ref. 12). We shall start the Fibonacci sequence with the seed element $F_0=A$, therefore $F_1=AB$, $F_2=ABA$, $F_3=ABAAB$, ... The Fibonacci sequences display the property $F_j = \{F_{j-1}, F_{j-2}\}$ for $j \geq 2$. Here we always refer to Fibonacci chains with 145 particles, corresponding to a Fibonacci generation index $j=10$, and with $d_A=3a$. Any Fibonacci chain subtends the periodic sequence obtained by setting $d_B=d_A$.

The eigenvalues and eigenvector of generalized eigenvalue problem (16) have been evaluated numerically by using LAPACK routines. Two cases are analyzed, one in which the equilibrium magnetization is parallel to chain axis and the other in which the equilibrium magnetization is orthogonal. The applied equilibrium magnetic field is parallel to the magnetization and has the same versus. When the equilibrium magnetization is longitudinally polarized the equilibrium is always stable whereas in the other case the equilibrium is stable only if the applied field is greater than a critical value depending on the chain geometry.

A. Ferromagnetic resonance frequencies

The ferromagnetic resonance frequencies depend on the effective external equilibrium field $h_{\text{eff}} \equiv h_0 + \kappa_{\text{an}}$, the equilibrium polarization, and the geometrical arrangement of the nanoparticles. In Fig. 1 we show the resonant frequencies normalized to the Kittel frequency, $\Omega_n \equiv \text{Re}\{\omega_n/h_{\text{eff}}\}$, versus the modal index n , for both the equilibrium polarizations and for two values of h_{eff} that also assure the stability of the transversally polarized equilibrium. We compare the resonance frequencies of the Fibonacci chain obtained by setting $d_B=1.5d_A$ with the resonance frequencies of the subtended periodic chain obtained by setting $d_B=d_A$.

In periodic chains the resonance frequencies cover almost continuously an interval, whose center and width depend on the equilibrium polarization, h_{eff} and a/d_A , with the exception of the two isolated highest values in the transverse equilibrium polarization and the two isolated lowest values in the longitudinal equilibrium polarization. They are the resonance frequency of the edge modes of the linear chain. As we shall see later these modes are localized at the two ends of the linear chains (e.g., Ref. 4). The edge modes and the corresponding isolated resonance frequencies arise in a periodic chain because the amplitude of the magnetic field due to the equilibrium magnetization at the ends of the chain is roughly half the amplitude of the magnetic field at the centers of the inner nanoparticles. For $d_A/a \rightarrow \infty$ the particles do not interact between them and it results $\Omega_n=1$ for any value h_{eff} . As the particle interaction becomes significant the resonance frequencies move away from the Kittel frequency and become different. For transverse equilibrium polarizations all the resonance frequencies become smaller than the Kittel fre-

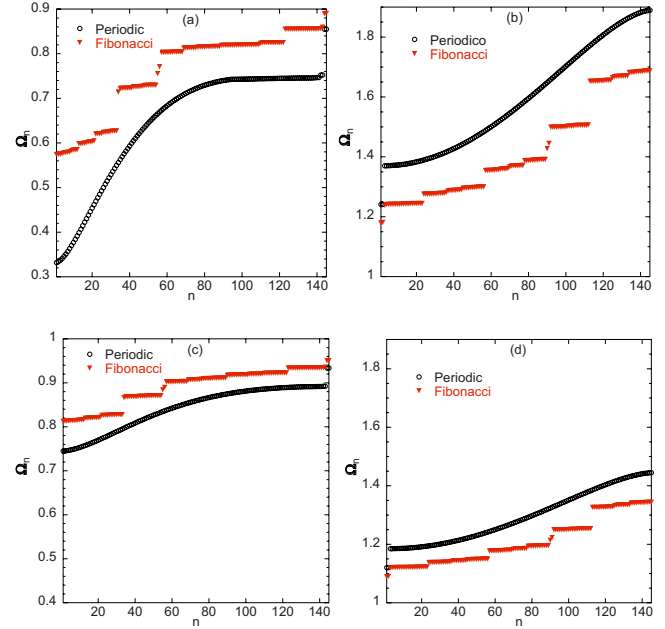


FIG. 1. (Color online) Ferromagnetic resonance frequencies in periodic ($d_A=3a$) and Fibonacci ($d_B=1.5d_A$) chains with 145 nanoparticles, normalized to the Kittel frequency, $\Omega_n \equiv \text{Re}\{\omega_n/h_{\text{eff}}\}$, versus the mode index n : transverse polarization with (a) $h_{\text{eff}}=0.1$ and (c) $h_{\text{eff}}=0.2$; longitudinal polarization with (b) $h_{\text{eff}}=0.1$ and (d) $h_{\text{eff}}=0.2$.

quency whereas for longitudinal equilibrium polarizations all the resonance frequencies become larger than the Kittel frequency. As the field h_{eff} increases the effects due to the interparticle interactions again becomes negligible and all resonance frequencies approach the Kittel frequency.

In Fibonacci chains many gaps arise in the discrete curve representing the resonance frequencies. In Fig. 1 we show the resonance frequencies obtained by setting $d_B/d_A=1.5$. For the transverse equilibrium polarization the gaps around $n=33$, $n=56$, $n=89$, and $n=122$ become wider as the ratio d_B/d_A increases. On the opposite, the remaining gaps become narrower and their width reduces to zero with increasing the d_B/d_A ratio. For the longitudinal equilibrium polarization the gaps around $n=23$, $n=56$, $n=89$, and $n=112$ become wider as the ratio d_B/d_A increases. On the opposite, the remaining gaps, as in transverse equilibrium polarization, become narrower and their width reduces to zero with increasing the d_B/d_A ratio. Furthermore, we observe that the gap widths decrease as h_{eff} increases.

The spectral gaps are a direct consequence of the aperiodic geometrical arrangement of the nanoparticles along the chain as in the quasi-periodic arrays of metallic nanoparticles.¹⁵ Indeed, the inner band gaps arise around the modal indexes that match the normalized spatial frequencies of the Fourier components of the Fibonacci sequence. In particular, the widest gaps arise around the modal indexes of the harmonics of the Fibonacci sequence with the largest amplitudes because of a strong spatial resonance.

For $d_B/d_A \geq 5$ the eigenvalues Ω_h tend to five values that depend on the effective field h_{eff} and the equilibrium polarization. In the Fibonacci chains with odd generation indexes

the resonant frequency additionally assumes the Kittel value. The origin of this degeneracy is the following. In the limit $d_B/d_A \rightarrow \infty$ the array becomes a chain of three types of isolated clusters. Indeed, since Fibonacci sequences are cube-free (e.g., Ref. 21), the symbol A can consecutively occur only one or two times while the symbol B occurs consecutively only once. As a consequence, for $d_B/d_A \rightarrow \infty$ we can only have clusters composed of at most one, two, or three particles. The number of degeneracy of each of the resonance frequencies is equal to the number of corresponding clusters in the chain. In addition, since Fibonacci sequences terminates with two alternating symbols (A or B) at each generation, in the Fibonacci sequences with odd generation indexes there is one isolated particle at the end of the chain (cluster B).

By summarizing, the above results clearly show the formation of large gaps at the modal indexes matching the normalized Fourier components of the Fibonacci sequence with the highest amplitudes. For values of d_B/d_A close to one, band gaps open due to the resonant coupling between the modes of the subtended periodic lattice and the Fourier components of the Fibonacci array with large amplitudes. For values of d_B/d_A much larger than one, the chain reduces to a set of noninteracting clusters composed of one, two, or three particles. In this case, the system has a strong degeneracy with four or five distinct natural frequencies, depending on the Fibonacci generation index being even or odd. Since the gaps may be widened by reducing the applied equilibrium magnetic field, in Fibonacci chains of magnetic nanoparticles we may obtain gap widths, normalized to the Kittel frequency, much greater than the plasmonic gap widths, normalized to the plasmon frequency, obtained in Fibonacci chains of metallic nanoparticles.

The 3 dB bandwidth normalized to the resonance frequency $\Delta\Omega_n$ and the quality factor Q_n of the n th mode are given by $2\alpha\omega_n^{(0)}(\mathbf{u}_n^{(0)}, \mathbf{u}_n^{(0)})$ and $2/\Delta\Omega_n$, respectively. For longitudinally polarized equilibria $\omega_n^{(0)}(\mathbf{u}_n^{(0)}, \mathbf{u}_n^{(0)})=1$; hence $\Delta\Omega_n=2\alpha$ and $Q_n=1/\alpha$ for any n . For transversally polarized equilibria $\omega_n^{(0)}(\mathbf{u}_n^{(0)}, \mathbf{u}_n^{(0)})$ may be greater than one if h_{eff} is very near the critical value separating stable and unstable equilibria; otherwise it is almost equal to one.

B. Dipolar modes

Now we study the dipolar modes of the linear chain. The localization character of the modes is described by the participation ratio defined as (e.g., Refs. 12 and 21)

$$P \equiv \frac{1}{2N} \frac{\|\mathbf{u}\|_2^2}{\|\mathbf{u}\|_4^4}, \quad (36)$$

where $\|\mathbf{u}\|_p = (\sum_{m=1}^{2N} |u_m|^p)^{1/p}$ is the p norm of the vector $\mathbf{u} \in \mathbb{C}^{2N}$. By choosing the normalization $\|\mathbf{u}\|_2=1$, the participation ratio yields a quantitative measure of the localization degree of the modes. If all the components of the mode \mathbf{u} are of the same order of magnitude (extended modes), the order of magnitude of all $|u_m|^2$ is $1/2N$ to satisfy the condition $\|\mathbf{u}\|_2=1$. As consequence the order of magnitude of all $|u_m|^4$ is $1/4N^2$ and the order of magnitude of $\|\mathbf{u}\|_4^4$ is $1/2N$. This means that the order of magnitude of the participation ratio

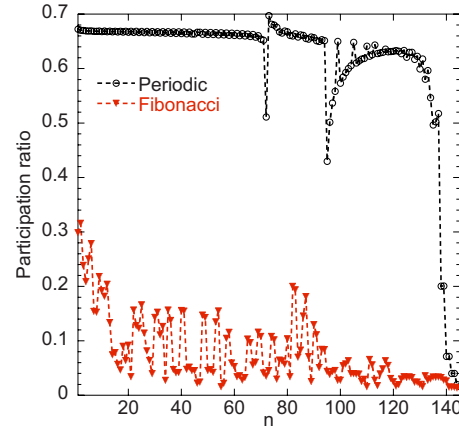


FIG. 2. (Color online) Participation ratio in periodic ($d_A=3a$) and Fibonacci ($d_B=1.5d_A$) chains with 145 nanoparticles and transversally polarized equilibrium.

of an extended mode is equal to one. Let us now consider a strongly localized mode, that is, the order of magnitude of the component u_M is much greater than the order of magnitude of all the other components of \mathbf{u} . The order of magnitude of u_M is equal to one to satisfy the condition $\|\mathbf{u}\|_2=1$; therefore the order of magnitude of $\|\mathbf{u}\|_4^4$ is equal to one, as well. This means that the order of magnitude of the participation ratio of strongly localized modes is equal to $1/2N$. Indeed, the participation ratio can take a value between $1/2N$ and 1. It gives a measure of the fraction of the particle number taken by the mode itself. The modes with smallest participation ratios are strongly localized.

Figure 2 shows the participation ratio versus the modal index n both for the Fibonacci chain with $d_B/d_A=1.5$ and the subtended periodic chain in the case of transverse equilibrium polarization. In the periodic chain the participation ratio is of the order of unity with the exception of few values corresponding to the modes that are strongly localized at the chain ends (edge modes), as we shall see later. All the modes in the Fibonacci chain have a participation ratio smaller than that of the modes in the subtended periodic chain. As the ratio d_B/d_A increases, the participation ratio strongly decreases and the modes become progressively more localized in different zones of the chain.

Figures 3 and 4 show the distribution along the chain of the real part of the y component of the magnetization of some modes, in order of decreasing participation ratio, both in the Fibonacci chain with $d_B/d_A=1.5$ (Fig. 4) and in the subtended periodic chain (Fig. 3), for the transverse equilibrium polarization.

In the periodic chain there exist three types of modes:⁴ “bulk” modes that are simply standing sine waves ($\sin[\pi p/(n+1)]$, where n denotes the mode index and p is the position index of the nanoparticle), Fig. 3(a); “ π -edge modes” characterized by a phase shift of π between adjacent dipoles that are close to the ends of the chain and exponentially decrease, Figs. 3(b) and 3(c); “bulk π modes” which are characterized by a periodic envelope, Fig. 3(b). The participation ratio of the bulk modes [Fig. 3(a)] is almost constant for $1 \leq n \leq 69$ and is roughly equal to 0.67 (this is the typical value for standing sine waves), Fig. 2. The 145th and

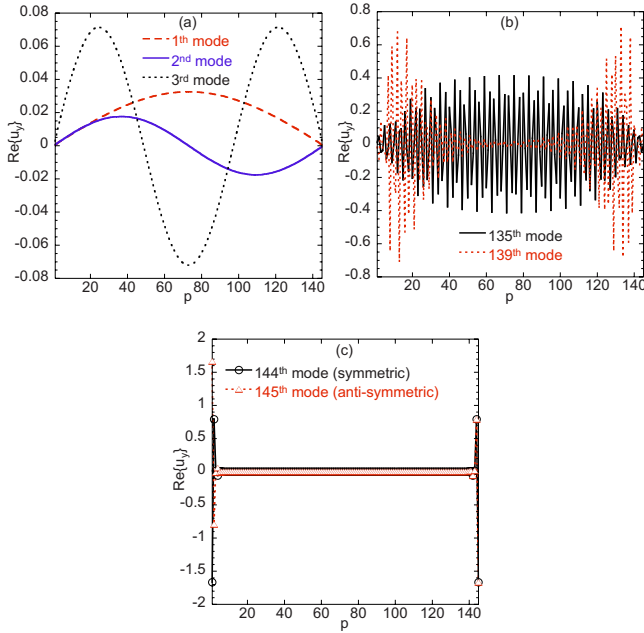


FIG. 3. (Color online) Real part of the y component of the dipole moment versus particle position index p in a periodic chain ($d_A=3a$) with transverse polarization, $N=145$ and $h_{\text{eff}}=0.1$: (a) bulk sine modes, (b) π bulk modes, and (c) π modes.

144th modes [Fig. 3(c)] are an example of π -edge antisymmetric and π -edge symmetric modes, respectively; they have the smallest values of the participation ratio, $P=0.02$. The transition between the bulk sine modes and π -edge modes

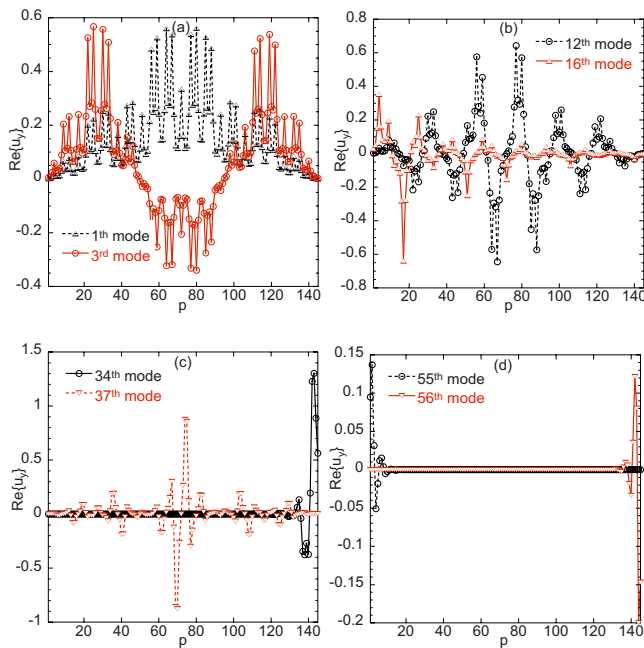


FIG. 4. (Color online) Real part of the y component of the dipole moments versus particle position index p in a linear Fibonacci chain ($d_A=3a$, $d_B=1.5d_A$) with transverse polarization, $N=145$ and $h_{\text{eff}}=0.1$: (a) bulk modes; (b) critical mode (12th mode) and a localized mode (16th mode); [(c) and (d)] strongly localized modes.

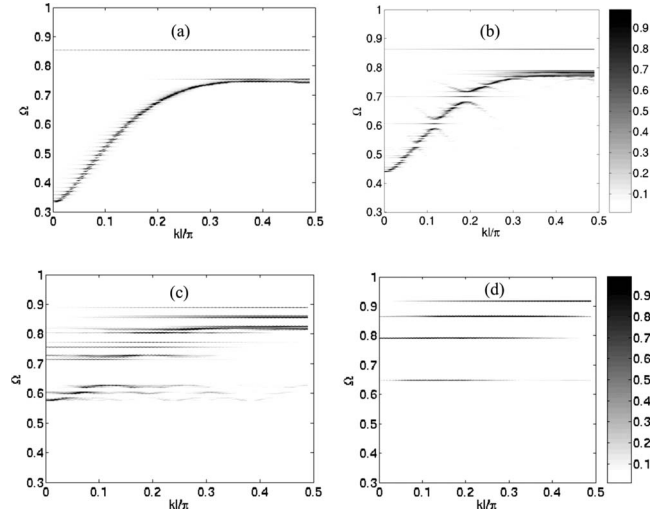


FIG. 5. Pseudodispersion diagrams for (a) periodic chain $d_A=3a$, and [(b)–(d)] quasi-periodic Fibonacci chain, (b) $d_B=1.1d_A$, (c) $d_B=1.5d_A$, and (d) $d_B=5d_A$, with transversally polarized equilibrium.

takes place gradually through the bulk π modes, Fig. 3(b). The participation ratio has two relative minima at $n=72$ and $n=95$ (Fig. 2). Unlike the edge modes, the 95th mode is shut up in the interior of the chain.

The first 11 modes in the Fibonacci chain are distributed bulk modes. Figure 4(a) shows the first mode ($P=0.30$) and the third mode ($P=0.24$). If we compare them with the corresponding modes of the subtended periodic chain [see Fig. 3(a)] we note that, even if the aperiodicity gives rise to a considerable distortion of the mode profiles, the qualitative behavior of the modes on the length scale of the chain resembles that of the periodic case. Figure 4(b) shows the characteristic features of the 12th mode ($P=0.20$), which separates the distributed bulk modes and the first-localized edge modes. The 16th mode is one of the first-localized edge modes ($P=0.06$). Figure 4(c) shows the 37th mode, which is a bulk localized mode ($P=0.05$) and the 34th mode, which is another edge mode, more localized than the previous ones ($P=0.03$). Figure 4(d) shows two strongly localized edge modes (the 55th and the 56th modes, which have $P=0.02$). Our findings show that many localized modes with very low participation ratio exist in chains of magnetic nanoparticles based on quasi-periodic Fibonacci order.

The band gaps which open in the Fibonacci chains can only be completely understood by studying the pseudodispersion diagrams of the modes (e.g., Refs. 12 and 21), as shown in Figs. 5 and 6 for transversally and longitudinally polarized equilibria, respectively. The pseudodispersion diagram associates to the real part of each natural frequency ω_n the intensity of the spatial Fourier transform of the corresponding eigenmode, which is represented on a black-white intensity scale. The real part of the natural frequencies of each mode, normalized to the Kittel frequency, is represented on the ordinate axis while the wave number k , normalized to π/l , where l is the chain length, is represented on the abscissa axis. The intensity of the Fourier components of each mode, calculated by the spatial Fourier transform, is represented on a black-white intensity scale.

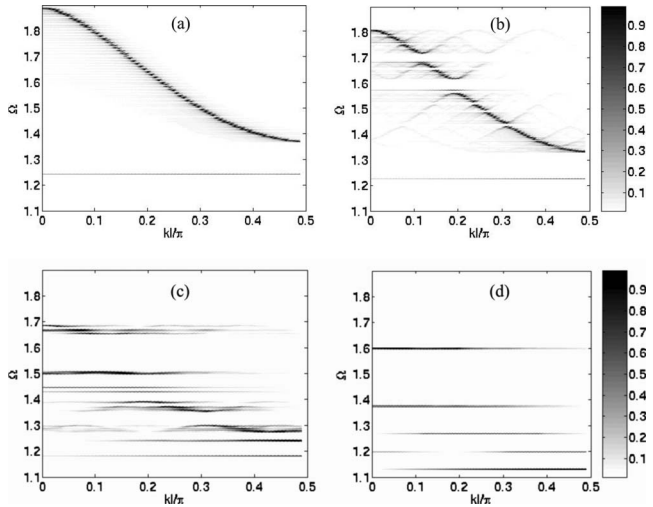


FIG. 6. Pseudodispersion diagrams for (a) periodic chain $d_A = 3a$, and [(b)–(d)] quasi-periodic Fibonacci chain, (b) $d_B = 1.1d_A$, (c) $d_B = 1.5d_A$, and (d) $d_B = 5d_A$, with longitudinally polarized equilibrium.

We show the pseudodispersion diagrams for several values of d_B/d_A [Figs. 5(a) and 6(a)]. The pseudodispersion curves for the periodic chains consist mainly of two branches, one corresponds to the bulk distributed modes and the other corresponds to the edge-localized modes (the straight lines parallel to the abscissa axis). Interestingly, in the chain with transversally polarized equilibrium the pseudodispersion curve relevant to the distributed modes increases monotonically across most of the pseudoBrillouin zones whereas in the chain with longitudinally polarized equilibrium it decreases monotonically. Therefore, the group velocity is positive in the chain with transversally polarized equilibriums and negative in the chain with longitudinally polarized equilibriums. The chain with longitudinally polarized equilibrium behaves as a medium with negative index of refraction. As d_B/d_A deviates from one, the dispersion curve breaks into several pseudogaps, as shown in Figs. 5(b) and 6(b). As d_B/d_A increases even further, the gaps widen until the branches of the dispersion curve reduce to a set of five segments parallel to the wave-vector axis, as shown in Figs. 5(d) and 6(d) (in the transversally polarized equilibrium the third and fourth segments are so close that they are not distinguishable). These diagrams show in a very clear way the principal spatial frequency of each eigenmode and underline that, while in the periodic lattice at each eigenmodes corresponds mainly one spatial frequency (with the exception of the edge modes), in the quasi-periodic case several wave numbers are excited due to the more spectral complexity of the subtended lattice. Moreover, these diagrams also show the formation of the gaps as the ratio d_B/d_A increases.

These results clearly demonstrate that the Fibonacci modulation of the coupling in magnetic nanoparticle chains is responsible for the gap formation in the pseudo-Brillouin zone, for both longitudinally and transversally polarized equilibriums.

A localized mode may be selectively excited by the time-varying external magnetic field if the difference between its

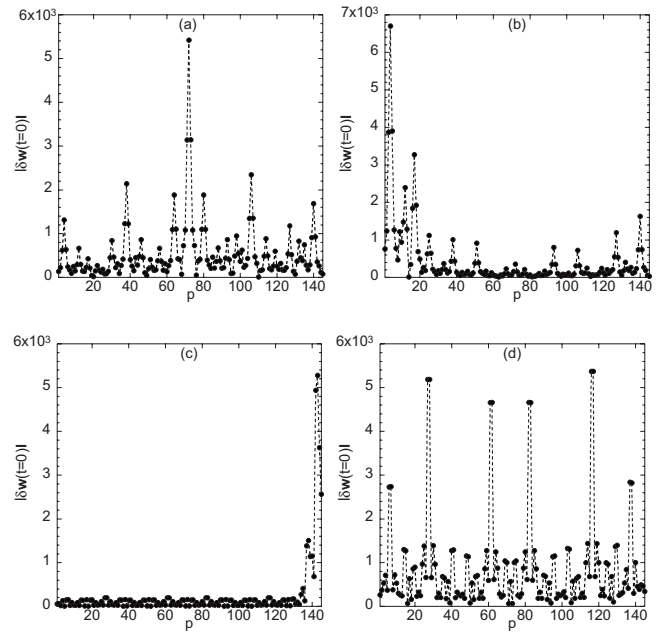


FIG. 7. Magnetization amplitude at $t=0$ versus the particle position index p induced by an external magnetic field varying sinusoidally in time in a linear Fibonacci chain with transverse equilibrium polarization, $d_A = 3a$, $d_B = 1.5d_A$, $N = 145$, $h_{\text{eff}} = 0.1$, and $\alpha = 10^{-3}$: the external field has a unitary-normalized amplitude and it is tuned on the resonance frequency of the (a) 17th, (b) 21th, (c) 34th, and (d) 45th modes.

resonance frequency and the resonance frequency of the adjacent mode is greater than the mean value of their 3 dB bandwidths. Figure 7 shows the distribution of the magnetization amplitude at $t=0$ induced by a uniform external magnetic field, varying sinusoidally in time, along a Fibonacci chain with $d_B = 1.5d_A$, $\alpha = 10^{-3}$, and a transverse equilibrium polarization. The external magnetic field is orthogonal both to the equilibrium field and to the chain axis, its normalized amplitude is equal to one and it is tuned on the resonance frequencies of the (a) 17th, (b) 21th, (c) 34th, and (d) 45th modes. The magnetization amplitude is of the order of the quality factor.

VI. CONCLUSIONS

In this paper we have investigated the spectral, localization, and dispersion properties of ferromagnetic dipolar modes, around a stable, saturated, and spatially uniform equilibrium in quasi-periodically modulated chains of magnetic nanoparticles based on the Fibonacci sequence. The evaluation of the natural frequencies and magnetization modes is reduced to the solution of a linear-generalized eigenvalue problem. We have demonstrated the presence of several band gaps in the pseudodispersion diagram of the Fibonacci chain and strongly localized magnetization oscillation modes. Future studies must be directed at extending the study beyond the simple dipolar interaction model considered here.

The presence of band gaps has a large influence on the

transport properties of these structures. They may have an impact in the design of new microwave devices, for example, microwave filters. The localized magnetization modes may provide an exciting opportunity to investigate static and dy-

namic magnetic properties on nanometric scales. They may have an impact in the design of new magnetic nanosensors and nanoscale magnetometers (tomography and magnetic imaging).

-
- ¹J. I. Martin, J. Nogués, Kai Liu, J. L. Vicent, and I. K. Schuller, *J. Magn. Magn. Mater.* **256**, 449 (2003).
- ²S. D. Bader, *Rev. Mod. Phys.* **78**, 1 (2006).
- ³R. Urban, A. Putilin, P. E. Wigen, S.-H. Liou, M. C. Cross, P. C. Hammel, and M. L. Roukes, *Phys. Rev. B* **73**, 212410 (2006).
- ⁴K. Rivkin, A. Heifitz, P. R. Sievert, and J. B. Ketterson, *Phys. Rev. B* **70**, 184410 (2004).
- ⁵P. Chu, D. L. Mills, and R. Arias, *Phys. Rev. B* **73**, 094405 (2006).
- ⁶K. Rivkin, Wentao Xu, L. E. De Long, V. V. Metlushko, B. Ilic, and J. B. Ketterson, *J. Magn. Magn. Mater.* **309**, 317 (2007).
- ⁷K. Rivkin, W. Saslow, V. Chandrasekhkar, L. E. De Long, and J. B. Ketterson, *Phys. Rev. B* **75**, 174408 (2007).
- ⁸L. Giovannini, F. Montoncello, and F. Nizzoli, *Phys. Rev. B* **75**, 024416 (2007).
- ⁹E. Maciá, *Rep. Prog. Phys.* **69**, 397 (2006).
- ¹⁰E. L. Albuquerque and M. G. Cottam, *Polaritons in Periodic and Quasi-Periodic Structure* (Elsevier, Amsterdam, 2004).
- ¹¹L. Dal Negro, C. J. Oton, Z. Gaburro, L. Pavesi, P. Johnson, A. Legendijk, R. Righini, M. Colocci, and D. S. Wiersma, *Phys. Rev. Lett.* **90**, 055501 (2003).
- ¹²L. Dal Negro and N. N. Feng, *Opt. Express* **15**, 14396 (2007).
- ¹³A. Gopinath, S. V. Boriskina, N. Feng, B. M. Reinhard, and L. Dal Negro, *Nano Lett.* **8**, 2423 (2008).
- ¹⁴A. Gopinath, S. V. Boriskina, B. M. Reinhard, and L. Dal Negro, *Opt. Express* **17**, 3741 (2009).
- ¹⁵C. Forestiere, G. Miano, G. Rubinacci, and L. Dal Negro, *Phys. Rev. B* **79**, 085404 (2009).
- ¹⁶M. d'Aquino, C. Forestiere, G. Miano, and C. Serpico, Joint European Magnetic Symposium 2008 (JEMS 08), Dublin, 14–19 September 2008 (unpublished).
- ¹⁷C. Forestiere, M. d'Aquino, G. Miano, and C. Serpico, *J. Appl. Phys.* **105**, 07D312 (2009).
- ¹⁸M. d'Aquino, C. Serpico, G. Miano, and G. Bertotti, *IEEE Trans. Magn.* **44**, 3141 (2008).
- ¹⁹S. I. Kiselev, J. C. Sankey, I. N. Krivorotov, N. C. Emley, R. J. Schoelkopf, R. A. Buhrman, and D. C. Ralph, *Nature (London)* **425**, 380 (2003).
- ²⁰W. H. Rippard, M. R. Pufall, S. Kaka, S. E. Russek, and T. J. Silva, *Phys. Rev. Lett.* **92**, 027201 (2004).
- ²¹C. Janot, *Quasicrystals: A Primer*, 2nd ed. (Oxford University Press, New York, 1997).